

Research of a UWB-Based Localization Algorithms

Liming Yao

School of Computer Science and Engineering
Xi'an Technological University
Xi'an, China
E-mail: 807255587@qq.com

Xiaohui Su

School of Computer Science and Engineering
Xi'an Technological University
Xi'an, China
E-mail: 287099144@qq.com

Yao Zhang

School of Computer Science and Engineering
Xi'an Technological University
Xi'an, China
E-mail: 2044828475@qq.com

Shuping Xu

School of Computer Science and Engineering
Xi'an Technological University
Xi'an, China
E-mail: 563937848@qq.com

Abstract—To address the problem of excessive outlier errors caused by noise in indoor non-line-of-sight (NLOS) environments—particularly in positioning and robot localization—two Chan–Taylor cooperative algorithms are proposed and implemented to suppress NLOS-induced errors. The first approach integrates Kalman filtering for error mitigation, while the second reconstructs distance measurements based on statistical characteristics. By combining multiple positioning algorithms, the proposed methods effectively reduce the impact of high noise levels and NLOS interference. Dynamic and static positioning tests were conducted to evaluate the accuracy of both schemes. The results indicate that localization errors in NLOS environments can be significantly reduced by both approaches, with the NLOS error suppression algorithm exhibiting superior performance and adaptability.

Keywords—Indoor Positioning; Non-Line-of-Sight (NLOS); Kalman Filter; Chan-Taylor Algorithm

I. INTRODUCTION

The demand for indoor positioning technologies has steadily increased due to the rapid development of mobile robotics. However, due to the inherent complexity and variability of indoor environments, obstacles and non-line-of-sight (NLOS) conditions are often unavoidable, leading to degraded positioning accuracy. Moreover, single localization algorithms often fail to achieve robust performance under such circumstances [1]. Ultra-Wideband (UWB) technology offers strong penetration capability, low power consumption, and high positioning

accuracy [2]. The Time Difference of Arrival (TDOA) technique, with its relatively low computational complexity, has become a widely used estimation method [3]. High localization accuracy is achieved under line-of-sight (LOS) conditions by the Chan algorithm, whereas its performance is significantly degraded in NLOS environments [4]. The Taylor algorithm [5] requires properly initialized values to ensure convergence; otherwise, the localization process may diverge. The cooperative Chan–Taylor approach [6], which takes the positioning result of the Chan algorithm as the initial value for the Taylor algorithm, can effectively guarantee the convergence of the localization process.

Numerous improvements targeting the deficiencies of UWB-TDOA indoor positioning systems (e.g., NLOS error interference and insufficient algorithm robustness) have been explored in existing studies. For instance, the Chan–Taylor cooperative localization method was adopted in [7], yet the study did not consider the impact of NLOS errors on positioning results. Reference [8] proposed a strategy to reject TDOA range data severely contaminated by NLOS effects based on residual analysis; this approach improved positioning accuracy to a certain extent but inevitably discarded part of the valid target-related information. Reference [9] distinguished LOS and NLOS propagation environments using a signal-to-noise ratio (SNR) threshold, but this method

requires determining an appropriate SNR-derived distance threshold, which increases the complexity of parameter tuning.

In this paper, based on TDOA technology, the Chan–Taylor cooperative algorithm is adopted to leverage the respective advantages of the Chan algorithm (high accuracy under LOS conditions) and the Taylor algorithm (high convergence stability with reasonable initial values), aiming to address the problem of degraded positioning performance under NLOS conditions. Two localization schemes with distinct technical paths are designed for NLOS error identification and mitigation: one integrates a Kalman filter to suppress random NLOS errors, and the other employs a distance reconstruction strategy to correct systematic NLOS biases. Subsequently, static and dynamic experiments are conducted to evaluate and compare the positioning performance of the two schemes in terms of key indicators such as root mean square error (RMSE), convergence rate, and robustness under different NLOS interference levels.

II. DESCRIPTION OF THE TDOA POSITIONING ALGORITHM

By selecting the first base station as the reference (master) station, a hyperbolic model can be established, and the Time Difference of Arrival (TDOA) can be expressed as:

$$r_{i,1} = r_i - r_1 = \sqrt{(x_i - x)^2 + (y_i - y)^2} - \sqrt{(x_1 - x)^2 + (y_1 - y)^2} \quad (1)$$

The variable $r_{i,1}$ is used to describe the discrepancy in distances, which is obtained by subtracting the distance from the target tag to the master station from the distance from the i -th base station to the same master station. Here, the target's real-world position is represented by the vector (x, y) , while the spatial location of the i -th base station is defined as (x_i, y_i) .

A. Chan Positioning Algorithm

The Chan algorithm is a non-iterative method for TDOA-based hyperbolic equation solving [10]. It employs a two-stage weighted least squares estimation to obtain target position. Under LOS

conditions with Gaussian noise, the algorithm exhibits low positioning error; however, its performance degrades significantly in NLOS environments.

B. Taylor Series Expansion Algorithm

An iterative technique, the Taylor algorithm necessitates a starting approximation [11]. The result obtained from the previous iteration serves as the initial value for the current one. By repeatedly applying the least squares method, the algorithm refines the estimated position until the error falls below a predefined threshold. Although this approach achieves high positioning accuracy, it is highly sensitive to the choice of initial values.

C. Fang Algorithm

In TDOA positioning applications where nonlinear equations need to be solved, the Fang algorithm offers a linearization approach as its core methodology; it linearizes the nonlinear positioning model and then solves the resulting linear equation system to derive the position coordinates of the target tag. This algorithm is characterized by straightforward implementation logic and low computational complexity. However, a key limitation is that it cannot exploit redundant observation information from base stations to optimize the target position solution, and it supports positioning with a maximum of three fixed base stations. Since the algorithm is unable to fully utilize the measurement data from more than three base stations, increasing the number of deployed base stations fails to yield further improvements in positioning accuracy.

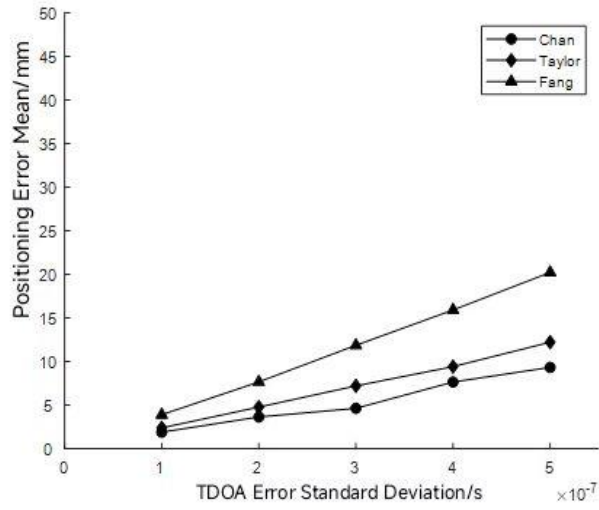
D. Performance Comparison of Various

Algorithms in a Gaussian Noise Environment

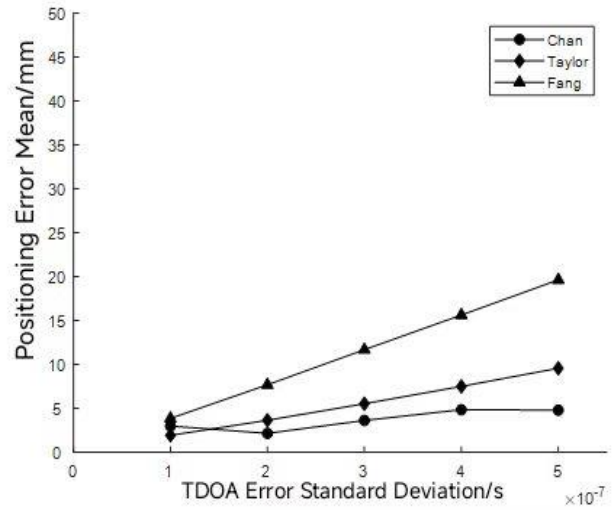
To compare the positioning performance of the Fang, Chan, and Taylor algorithms in an indoor line-of-sight (LOS) environment, a combined experiment and simulation study was carried out in this paper. Specifically, the linear distance between adjacent base stations was configured to 5 m, and 4 – 7 fixed base stations were randomly deployed for Time Difference of Arrival (TDOA) data acquisition. For the performance comparison, two constraints were imposed: first, only the positioning error induced by system equipment was considered; second, the scenario was

restricted to three positioning base stations for positioning calculation. The measurement error was assumed to follow a zero-mean Gaussian distribution with standard deviations of 0.1, 0.2,

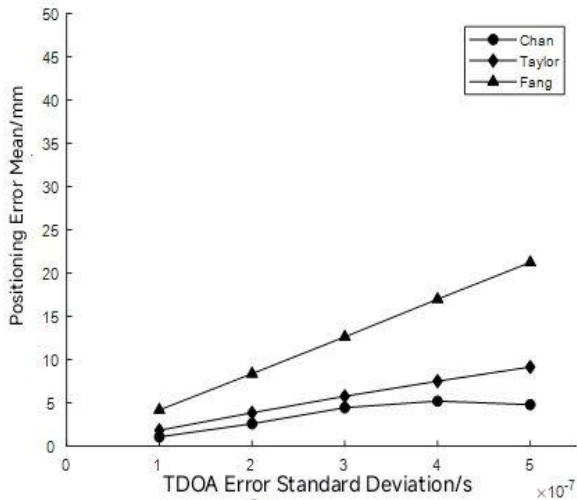
0.3, 0.4, and 0.5 μ s, respectively. The simulation results derived from the experimental parameter settings are presented in Figure 1.



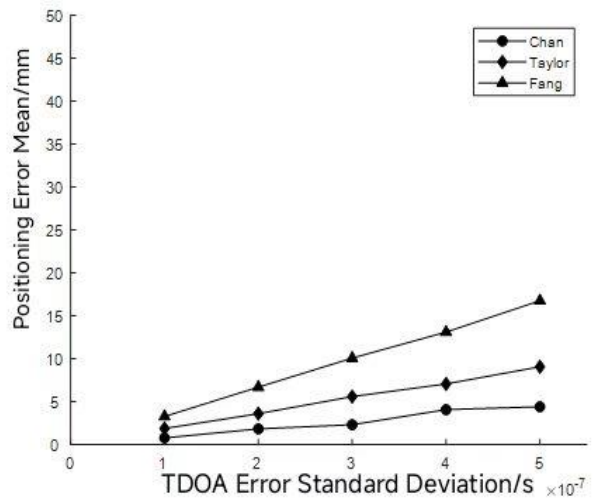
(a) 4 base stations



(c) 6 base stations



(b) 5 base stations



(d) 7 Base Station

Figure 1. Comparison of different base station performances among three algorithms

As illustrated in Figure 1, under the constraint of three base stations in the indoor LOS environment, the positioning performance of the three algorithms exhibits significant differences. Specifically, the Chan algorithm achieves the highest positioning accuracy (with the smallest root mean square error, RMSE), followed by the Taylor algorithm, while the Fang algorithm yields

the largest positioning error. This result is consistent with the inherent characteristics of the algorithms: unlike the Fang algorithm, which is limited to utilizing information from at most three base stations and cannot exploit redundant observation data, the Chan algorithm and the Taylor algorithm can fully leverage the TDOA observation information from base stations. This

enables them to optimize the target position estimation result and thus achieve superior positioning performance.

E. Chan–Taylor Cooperative Localization Algorithm

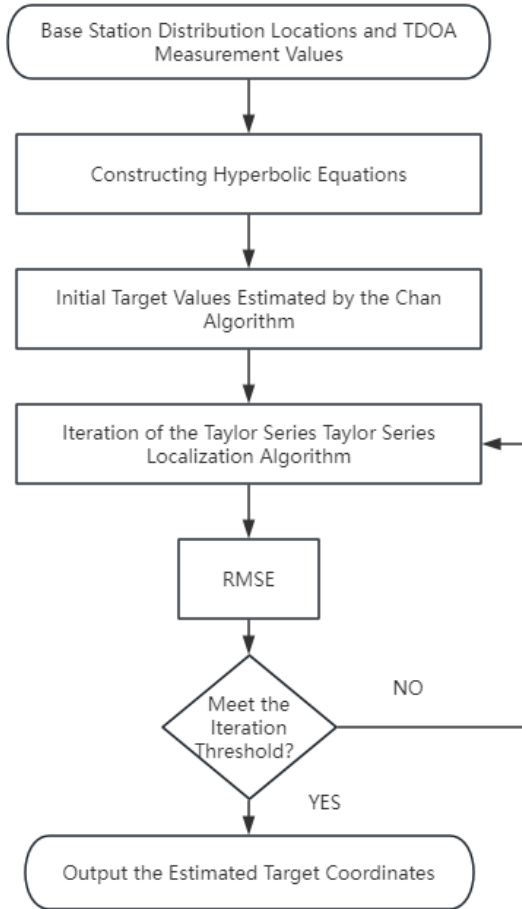


Figure 2. Flowchart of the Chan–Taylor Cooperative Algorithm

The location result produced by the Chan method serves as the starting point for the Taylor procedure, in which the estimate is progressively improved via repeated least-squares corrections until the residual error satisfies a preset criterion. The iteration is terminated when the convergence criterion is met, and the algorithm outputs a more accurate position estimate.

III. NLOS ERROR IDENTIFICATION

Under NLOS (non-line-of-sight) conditions, the signal from the tag experiences an additional propagation delay when reaching the base station, resulting in a positive bias. At epoch t_i , the

mathematical model characterizing the range measurement discrepancies between the target and the base station is formulated as follows [12]:

$$r_m(t_i) = d_m(t_i) + n_m(t_i) + NLOS_m(t_i), i = 1, 2, \dots, k \quad (2)$$

$$d_m(t_i) = \sqrt{(x_i - x_m)^2 + (y_i - y_m)^2} \quad (3)$$

At time t_i , the value $r_m(t_i)$ refers to the distance measured between the base station and the tag when the signal propagates through non-line-of-sight (NLOS) environments, while $d_m(t_i)$ stands for the actual distance from the base station to the tag under line-of-sight (LOS) conditions, $n_m(t_i)$ refers to the system measurement error; and $NLOS_m(t_i)$ is the ranging error caused by the NLOS environment at time t_i . A smoothing operation is performed on the ranging data from the tag to each base station, from which the following relationship is derived.

$$r_m(t_i) = \sum_{n=1}^{N-1} a_m(n) t_i^n \quad (4)$$

In equation (4), the order of the polynomial is $N-1$, and the polynomial coefficients $\{a_m(n)\}$ can be obtained using the least squares method.

Assuming the resulting coefficients are $\{\hat{a}_m(n)\}$, the smoothed system measurement value can be expressed as:

$$s_m(t_i) = \sum_{n=1}^{N-1} \hat{a}_m(n) t_i^n \quad (5)$$

The sample standard deviation of $r_m(t_i)$ can then be calculated and is expressed as:

$$\delta_m = \sqrt{\frac{1}{k} \sum_{i=0}^{k-1} (s_m(t_i) - r_m(t_i))^2} \quad (6)$$

In equation (6), the number of ranging samples is denoted by k . As can be seen from equation (2), the system measurement data contain both errors due to NLOS signal propagation and measurement noise. Therefore, the standard deviation of the raw

measurements is greater than that of the smoothed values.

Assuming that the system error's standard deviation measurement error from the tag to the m -th base station under LOS conditions is δ_m and that multiple measurements under LOS conditions yield δ_m , the presence of NLOS propagation can be determined using the difference between $\hat{\delta}_m$ and δ_m :

$$\begin{cases} H_0 : \delta_m = \delta_m, LOS \\ H_1 : \delta_m > \delta_m, NLOS \end{cases} \quad (7)$$

The residual value:

$$e_m(t_i) = r_m(t_i) - d_m(t_i) \quad (8)$$

Once the measurement error under NLOS conditions is identified, it is optimized using a Kalman filter, and the target's optimal estimated position is then determined using the positioning algorithm.

IV. SUPPRESSION AND RECONSTRUCTION OF NLOS ERRORS

A. Kalman Filter-Based Suppression Algorithm

The Kalman filter can effectively smooth the data, reducing the impact of outliers. When NLOS errors are present, the ranging residuals can be incorporated into the Kalman filter computation at the next time step. According to equation (8), the ranging residual can be denoted as $C = e_m(t_i)$, and the Kalman filter update formula that accounts for the non-zero residual is expressed as:

The estimated measurement observation vector Y_k is expressed as:

$$Y_{k/k-1} = H_{k/k-1} X_{k/k-1} + C \quad (9)$$

The difference between Y_k and the estimated value $Y_{k/k-1}$ is:

$$e_{k/k-1} = Y_k - Y_{k/k-1} = Y_k - H_k X_{k/k-1} - C \quad (10)$$

The state vector $\hat{X}_{k/k-1}$ is corrected using the error $e_{k/k-1}$,

$$\hat{X}_{k/k-1} = \hat{X}_{k/k-1} + K_k (Y_k - H_k \hat{X}_{k/k-1} - C) \quad (11)$$

In NLOS environments, a novel Kalman filter can be expressed as:

$$\hat{X}_{k/k-1} = A X_{k-1/k-1} \quad (12)$$

$$P_{k/k-1} = A P_{k-1/k-1} A^T + \Gamma_{k,k-1} Q_{k,k-1} \Gamma_{k,k-1}^T \quad (13)$$

$$K_k = P_{k-1/k-1} H_k^T [H_k P_{k-1/k-1} H_k^T + R_k]^{-1} \quad (14)$$

$$\hat{X}_{k/k-1} = \hat{X}_{k/k-1} + K_k (Y_k - H_k \hat{X}_{k/k-1} - C) \quad (15)$$

$$P_{k/k-1} = [I - K_k H_k] P_{k-1/k-1} \quad (16)$$

According to reference [13], the state vector is defined as $X_k = [r_k \quad v_{rk}]^T$, $A = \begin{bmatrix} 1 & T \\ 0 & 1 \end{bmatrix}$, $H_k = [1 \quad 0]$, r_k represents the ranges from the moving tag to each base station, and v_{rk} representing the velocity of the moving tag relative to the base stations. (T) is the time interval, $\Gamma_{k,k-1}$ denotes the state noise coefficient matrix, and Q denotes the covariance matrix of the process noise, K_k represents the Kalman gain, and I denotes the identity matrix.

The new Kalman filter is used to perform LOS-based optimization and reconstruction of the measurement data in NLOS environments. The reconstructed LOS-optimized data is then input into the Chan-Taylor cooperative algorithm for further localization processing, ultimately yielding the optimal target position.

B. NLOS Error Distance Reconstruction Algorithm

Since the motion of a moving tag is a continuous process, the state at the current time can be represented using the state from the previous time step [14]. In the distance reconstruction-based algorithm, the NLOS distance is reconstructed using the distance value under LOS conditions from the previous time step

and the distance change rate. The distance at step k is expressed based on its value at step $k-1$, as given below:

$$\tilde{r}_i^k = d_i^{k-1} d_i^{k-1} T + n_i^k \quad (17)$$

In equation (17), \tilde{r}_i^k represents the reconstructed distance under NLOS conditions, the system error associated with the tag and base station i at time (k) is denoted by n_i^k , and d_i^{k-1} represents the rate of change of the range from the tag to the i -th base station at time $k-1$.

$$d_i^k = \frac{\partial d_i^k}{\partial T} \quad (18)$$

$$d_i^k = \frac{\{(X_m^{k-1})^2 + (Y_m^{k-1})^2\} T + X_m^{k-1}(X_i - X_m^k) + Y_m^{k-1}(Y_i - Y_m^k)}{\sqrt{(X_i - X_m^k)^2 + (Y_i - Y_m^k)^2}} \quad (19)$$

In summary, to obtain the distance information at the current time, it is necessary to know the distance from the previous time step as well as the state information of the moving tag. The reconstructed distances under NLOS conditions are then fed into the Chan-Taylor cooperative method to derive the final location estimate.

V. EXPERIMENTAL ANALYSIS

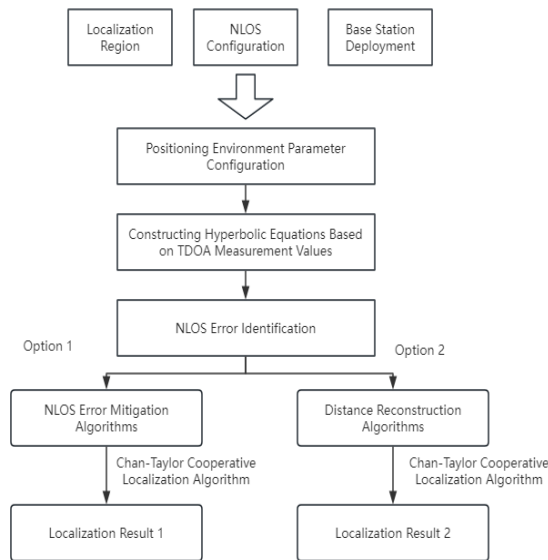


Figure 3. Experimental Setup

An $8\text{ m} \times 8\text{ m}$ complex indoor NLOS environment was selected, with three base stations randomly placed at non-uniform coordinates denoted as B0, B1, and B2. Data were collected at a frequency of 0.15 s, with approximately 100 samples per coordinate point. In the static scenario, localization was performed at four different coordinate points, while in the dynamic scenario, the actual trajectory of a mobile robot was tracked. Two NLOS error suppression schemes were applied to analyze the localization results based on the measured observation data. The experimental testing and analysis procedure is illustrated in Figure 3.

A. Static Positioning Results and Analysis

The static positioning results of the two schemes are presented in Figures 4–7.

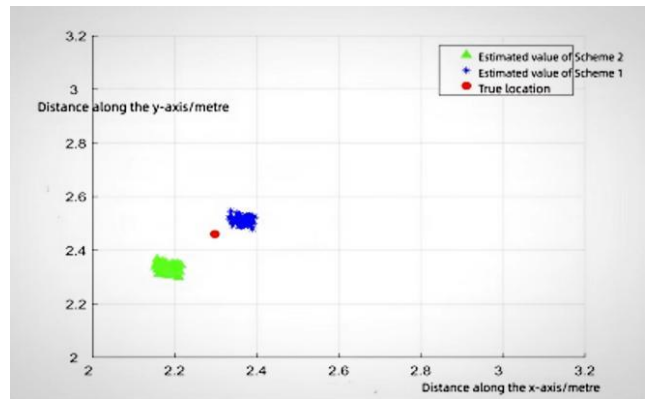


Figure 4. Test Point T1 (2.3, 2.53)

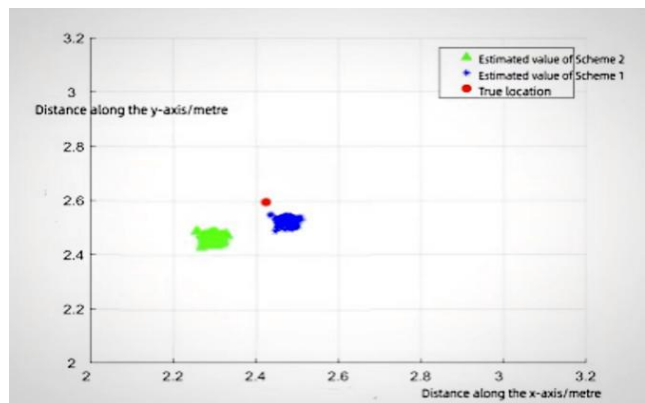


Figure 5. Test Point T2 (2.42, 2.6)

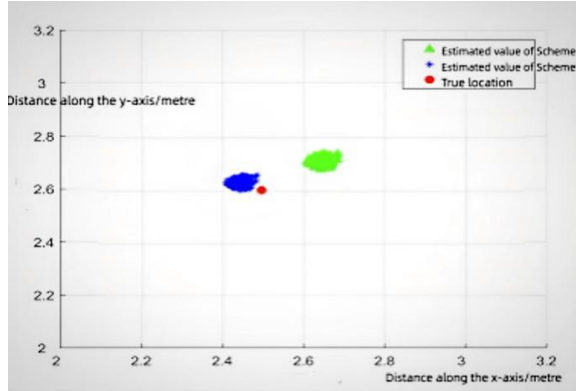


Figure 6. Test Point T3 (2.5, 2.6)

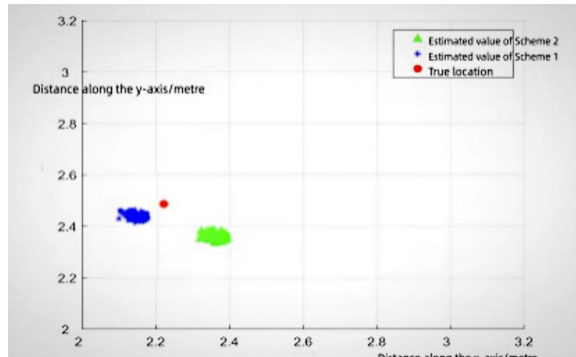


Figure 7. Test Point T4 (2.22, 2.5)

TABLE I. STATIC POSITIONING ACCURACY RESULTS OF THE TWO SCHEMES (M)

Tag	Test Point	IRMSE	2RMSE
T1	(2.3, 2.53)	0.052	0.103
T2	(2.42, 2.6)	0.045	0.095
T3	(2.5, 2.6)	0.039	0.087
T4	(2.22, 2.5)	0.041	0.112

As shown in Figures 4 - 7, the positioning accuracy at the four test points is noticeably higher for Scheme 1 compared to Scheme 2. Moreover, Table 1 shows that Scheme 1 achieves a substantially smaller RMSE compared with Scheme 2, demonstrating superior localization performance.

B. Statistical Characteristic Analysis of Static Positioning Results

To further quantify the positioning stability and data dispersion characteristics of the two schemes, the standard deviation (SD) and 95% confidence interval (CI) of static positioning were additionally calculated. These indicators can be used in addition to the root mean square error (RMSE) to supplement the evaluation dimensions in terms of

error dispersion and result credibility range, thereby facilitating a more comprehensive and objective assessment of the reliability and consistency of the positioning results.

TABLE II. THE STATIC POSITIONING STATISTICS INDICATORS OF SCHEME 1

	RMSE	SD	95% confidence interval
T1(2.3,2.53)	0.052	0.012	[0.048,0.056]
T2(2.42,2.6)	0.045	0.010	[0.042,0.048]
T3(2.5, 2.6)	0.039	0.008	[0.037,0.041]
T4(2.22,2.5)	0.041	0.009	[0.038,0.044]
average value	0.044	0.010	[0.042,0.046]

TABLE III. THE STATIC POSITIONING STATISTICS INDICATORS OF SCHEME 2

	RMSE	SD	95% confidence interval
T1(2.3,2.53)	0.103	0.028	[0.095,0.111]
T2(2.42, 2.6)	0.095	0.025	[0.089,0.101]
T3(2.5, 2.6)	0.087	0.023	[0.082,0.092]
T4(2.22, 2.5)	0.112	0.031	[0.104,0.120]
average value	0.099	0.027	[0.094,0.104]

As shown in the above table, it can be seen that Scheme 1 demonstrates significant advantages in terms of stability and reliability. Its standard deviation (SD = 0.008 - 0.012) is much smaller than that of Scheme 2 (SD = 0.023 - 0.031), indicating that the positioning results of Scheme 1 are more concentrated and less affected by random noise; the 95% confidence interval of Scheme 1 is narrower, implying that the true positioning error is more likely to fall within a smaller range, thus ensuring. This fully verifies that the Kalman filter can effectively suppress abnormal values caused by non-line-of-sight (NLOS) and improve the positioning results.

C. Comparison of Dynamic Positioning Results with Quantitative Statistics

As shown in Figures 8 and 9, the trajectory of Scheme 1 aligns more closely with the true trajectory, and its cumulative distribution function at an error of 20 cm is higher than that of Scheme 2, indicating better positioning accuracy. Figures 10, 11, and 12 additionally show that Scheme 1 yields smaller distance errors between the target and the base stations.

In summary, both Scheme 1 and Scheme 2 can mitigate localization errors in NLOS environments,

meeting general positioning requirements. However, Scheme 1 provides higher positioning accuracy and is better suited for scenarios demanding precise localization.

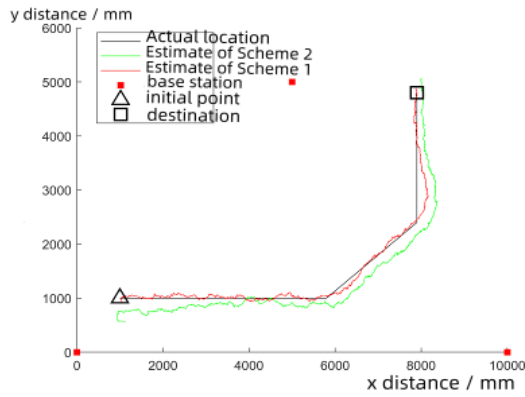


Figure 8. Dynamic Trajectories of the Two Schemes

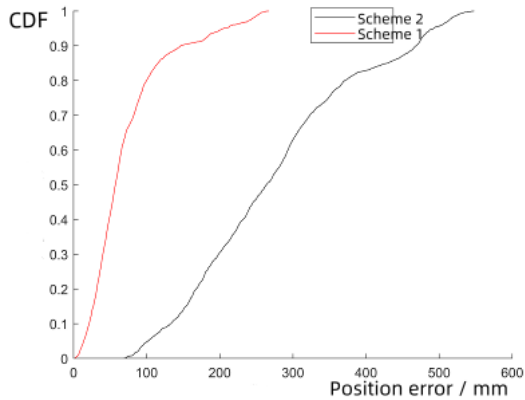


Figure 9. CDF of the Positioning Trajectories for the Two Schemes

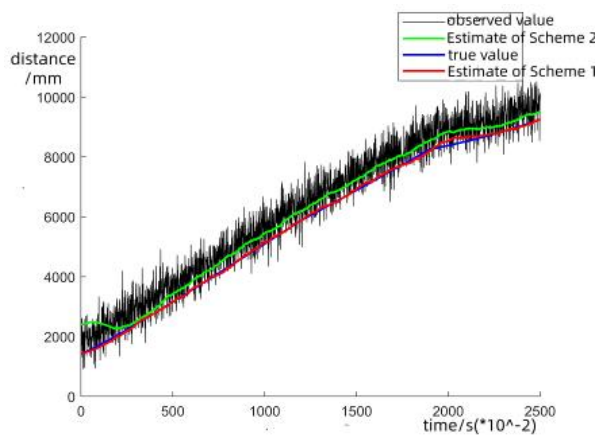


Figure 10. Distances Between the Target and the First Base Station for the Two Schemes

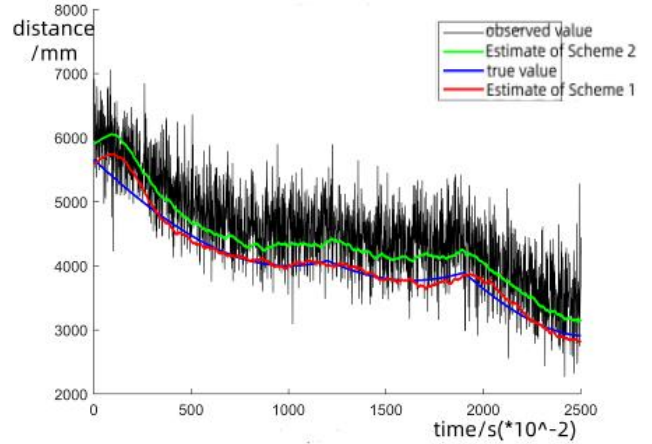


Figure 11. Distances Between the Target and the Second Base Station for the Two Schemes

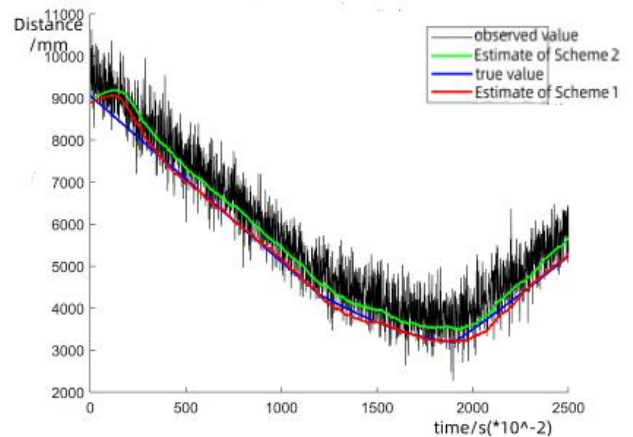


Figure 12. Distances Between the Target and the Third Base Station for the Two Schemes

D. Comparison of Chan – Taylor with Mainstream Single-Point Positioning Algorithms

The experiment was conducted in a $8m \times 8m$ complex indoor NLOS environment. Three base stations were randomly and unevenly arranged and labeled as B0, B1, and B2. A positioning model was constructed based on TDOA technology. In the area with relatively small positioning errors, a point was randomly selected as the simulation coordinate for positioning. The selected coordinate was (5.45, 5.25), as shown in Figure 13 below.

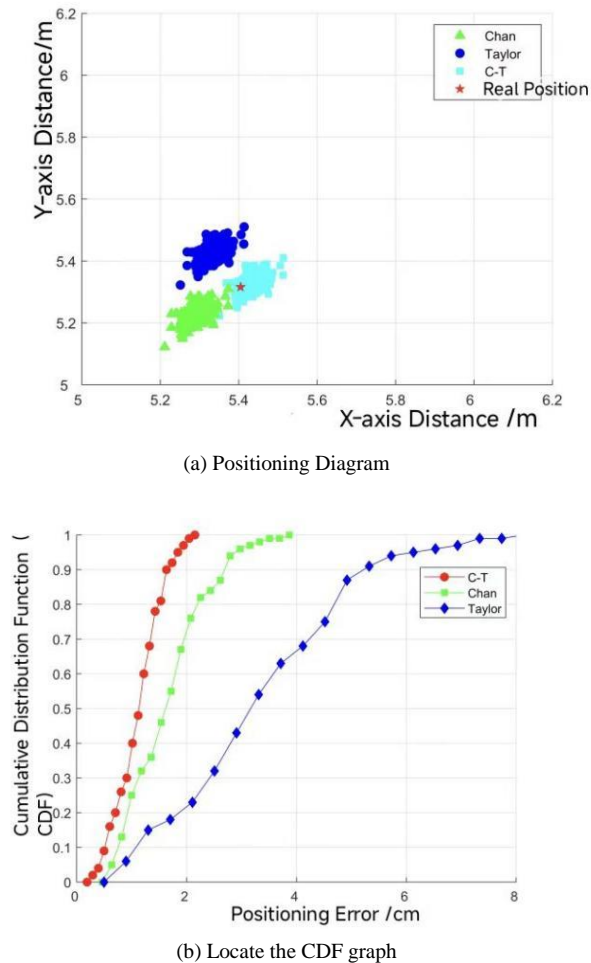


Figure 13. The positioning results of each algorithm at the coordinates (5.43, 5.79)

As is evident from Figure 13(a), the path determined by the C-T collaborative algorithm is more consistent with the true position when compared to traditional methods, suggesting that the C-T collaborative positioning approach outperforms both the Chan algorithm and the Taylor algorithm in terms of positioning performance. Additionally, when examining the static positioning performance through Figure 13(b), it is found that the root mean square error of the C-T collaborative method covers roughly 95% of the data points, whereas the Chan algorithm only achieves 78%. This discrepancy could be attributed to the unsuitable choice of initial parameters. Meanwhile, the Taylor algorithm shows a static positioning error rate of 22%. In contrast to the Taylor algorithm, which exhibits a 22% error rate, the C-T collaborative positioning

algorithm demonstrates a notable improvement by effectively minimizing positioning inaccuracies when compared to both the Chan algorithm and the Taylor algorithm.

VI. CONCLUSIONS

In complex and dynamic indoor environments, the raw observations obtained by TDOA measurements are subject to NLOS errors and high-frequency noise, which can significantly degrade the positioning accuracy of indoor mobile robots. This study employs the Chan–Taylor cooperative localization algorithm along with NLOS error identification, and proposes two schemes—one based on Kalman filtering and the other on distance reconstruction using statistical characteristics—to process outliers in the observation data and mitigate NLOS errors, thereby improving localization accuracy. Both schemes are capable of suppressing NLOS errors to a certain extent; however, more pronounced improvements in positioning accuracy are achieved by Scheme 1, offering valuable guidance for high-precision localization of indoor mobile robots.

ACKNOWLEDGMENT

The authors wish to thank the cooperators. This research is partially funded by the Project funds in Shaanxi province University Student Innovation and Entrepreneurship Fund Projects Indoor personnel positioning and detection equipment (S202510702093X) and Multi-source tightly-coupled SLAM system for autonomous driving (S202510702092).

REFERENCES

- [1] LIU Cong-feng, YANG Jie, WANG Feng-shuai. Joint TDOA and AOA location algorithm [J]. Journal of Systems Engineering & Electronics, 2013, 24(2):183-188.
- [2] LIU Fei, LI Xin, WANG Jian, ZHANG Ji-xian. An Adaptive UWB/MEMS-IMU Complementary Kalman Filter for Indoor Location in NLOS Environment [J]. Remote Sensing, 2019, 11(22):1-21.
- [3] Yang Yu, et al. Positioning Optimization Methods Using TOA/TDOA Under NLOS Conditions[D]. Chengdu: University of Electronic Science and Technology of China, 2018:11-12.
- [4] Chan Y T, Ho K C. A simple and efficient estimator for hyperbolic location[J]. IEEE Transactions on Signal Processing, 1994, 42(8): P.1905-1915.
- [5] Wylie M R, Holtzman J. The Non-Line of Sight Problems in Mobile Location Estimate[C]. IEEE

- International Conference on Universal Personal Communications, 1996: 827-831.
- [6] HUA Cheng, ZHAO Kun, DONG Danan, et al. Multipath Map Method for TDOA Based Indoor Reverse Positioning System with Improved Chan-Taylor Algorithm[J]. Sensors, 2020, 20(11):3223.
- [7] YANG Jun-feng, ZHANG Pi-zhuang, et al. Time Difference of Arrival Localization Based on Chan Algorithm and Taylor Series Algorithm[J]. Nuclear Electronics & Detection Technology, 2013, 33(04):480-482+526.
- [8] WANG Ruirong, ZHENG Shuwan, CHEN Haolong, XUE Chu, et al. An Cooperative Localization Method Based on Taylor and Kalman Algorithms[J]. Chinese Journal of Sensors and Actuators, 2014, 27(11):1557-1561.
- [9] YAN Bao-fang, MAO Qing-zhou, et al. An UWB indoor positioning algorithm based on Kalman filtering[J]. Transducer and Microsystem Technologies, 2017, 36(10):137-140+143.
- [10] Chan Y T, Hang H, Ching P C. Exact and Approximate Maximum Likelihood Localization Algorithms[J]. IEEE Transactions on Vehicular Technology Vt, 2006, 55(1): 10-16.
- [11] Guo Ming-tao, Li Wen-yuan, Gong Fu-chun, et al. Modified Taylor Series Position Algorithm in the Indoor Environment[J]. Wireless Communication Technology, 2009, 1:2656-2660.
- [12] Gao Xiang-jian. UWB Indoor Localization System[D]. The George Washington University. 2018.
- [13] Nozarian S, Dehghan Y, Janhan M V. Solving TSP on the Basis of Grid and Genetic Algorithm[J]. International Proceedings of Computer Science & Information Tech, 2012, 34: 61-66.
- [14] Xuan Wei. UWB Localization with LOS/NLOS Range Measurement[D]. Hangzhou Dianzi University, 2020.